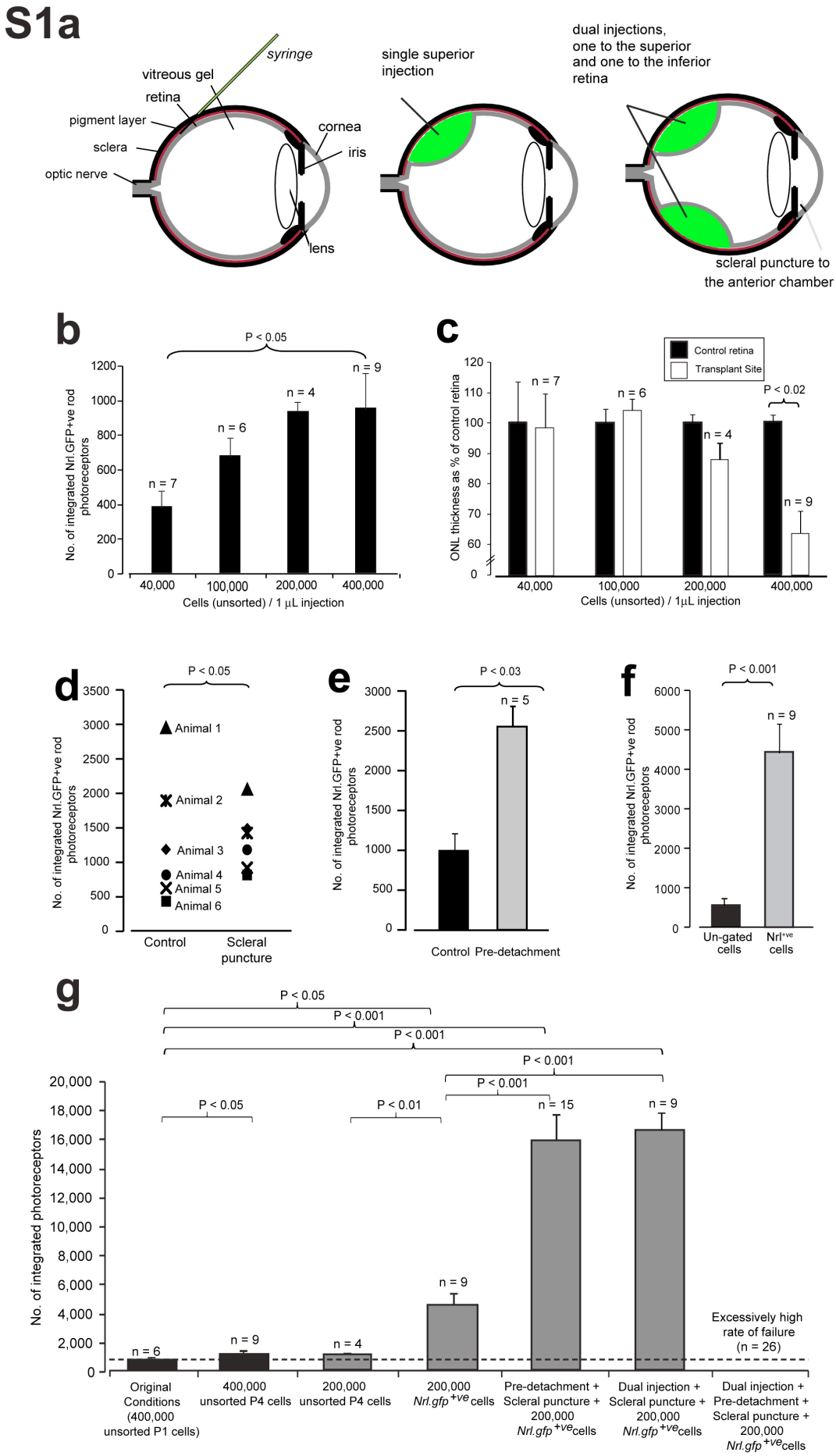
S1a
syringe
vitreous gel
retina
pigment layer
sclera
optic nerve
cornea
iris
lens
single superior injection
dual injections, one to the superior and one to the inferior retina
scleral puncture to the anterior chamber
b
P < 0.05
n = 7
n = 6
n = 4
n = 9
No. of integrated Nrl.GFP+ve rod photoreceptors
Cells (unsorted) / 1 µL injection
c
Control retina
Transplant Site
P < 0.02
ONL thickness as % of control retina
d
P < 0.05
Animal 1
Animal 2
Animal 3
Animal 4
Animal 5
Animal 6
Control
Scleral puncture
e
P < 0.03
n = 5
Control
Pre-detachment
f
P < 0.001
n = 9
Un-gated cells
Nrl+ve cells
g
P < 0.05
P < 0.001
P < 0.001
P < 0.001
P < 0.001
P < 0.05
P < 0.01
n = 15
n = 9
n = 9
n = 6
n = 9
n = 4
Excessively high rate of failure (n = 26)
No. of integrated photoreceptors
Original Conditions (400,000 unsorted P1 cells)
400,000 unsorted P4 cells
200,000 unsorted P4 cells
200,000 Nrl.gfp+ve cells
Pre-detachment + Scleral puncture + 200,000 Nrl.gfp+ve cells
Dual injection + Scleral puncture + 200,000 Nrl.gfp+ve cells
Dual injection + Pre-detachment + Scleral puncture + 200,000 Nrl.gfp+ve cells

Supplementary Figure 1. Improvements in the transplant procedure lead to significant improvements in photoreceptor integration into the adult wildtype retina. a, schematic showing changes to the transplantation procedure including single and dual injections and scleral puncture to the anterior chamber. **b, c,** the number of donor cells injected per μL had a significant impact both on the number of integrated photoreceptors (**b**) and the survival of endogenous photoreceptors (**c**) following a single subretinal transplant of unsorted P1 retinal cells. The loss of the endogenous ONL with higher concentrations of cells injected is likely to be due to a greater number of donor cells remaining in the subretinal space, causing a prolonged detachment and subsequent cell death in the underlying ONL. Data are mean ± s.e.m; ANOVA with tukey's correction for multiple comparisons (b) or paired t-test (c); n = animals. **d,** a puncture to the anterior chamber prior to cell transplantation reduced the variability between individuals although had no overall effect on cell integration. Data are mean ± s.e.m; F-test. **e,** pre-detachment of the retina 48hrs prior to cell transplantation had a modest effect on subsequent integration (see also [4]); mean± s.e.m; paired t-test; n = animals . **f,** purification of the donor cell population had by far the greatest impact on photoreceptor integration. Histogram shows comparison between un-gated (passed through FACs machine but not sorted for GFP) cells with *Nrl.GFP*$^{+ve}$-rod-precursors. mean± s.e.m; paired t-test; n = animals. N.B. data in b-e is from unsorted donors. **g,** histogram summarising the impact of the above manipulations to the transplant procedure, including donor age (P1 versus P4), purifying the donor cell population to include only *Nrl.GFP*$^{+ve}$-rod-precursors, surgical manipulations including pre-detachment of the retina 48 hrs prior to injection, scleral puncture to the anterior chamber to introduce a deflation and minimise reflux, dual injections to superior and inferior retina and combinations of these techniques. Mean ± s.e.m; ANOVA with tukey's correction for multiple comparisons; n = eyes.

S2

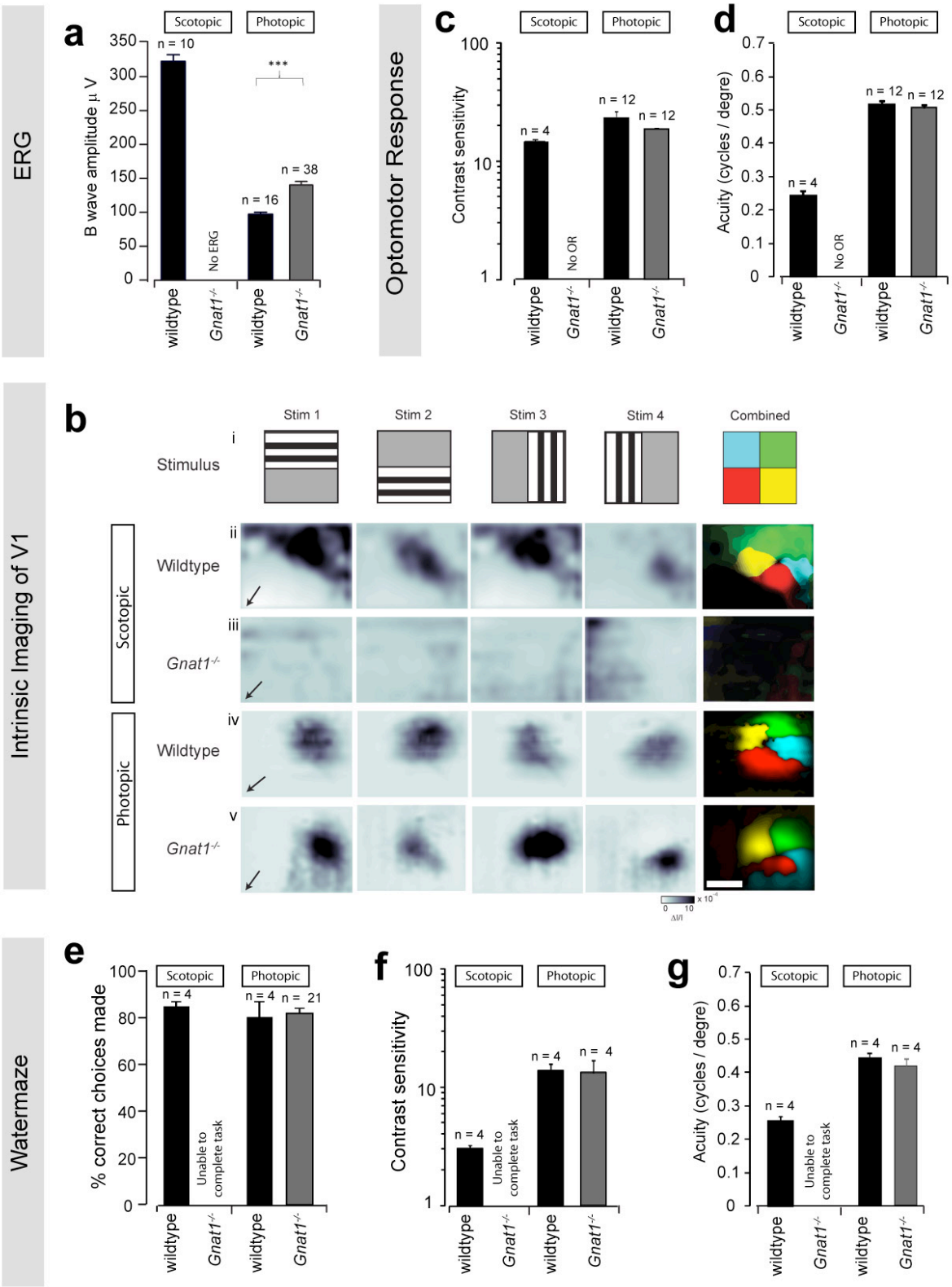
ERG
a
Scotopic
Photopic
B wave amplitude µ V
n = 10
No ERG
n = 16
n = 38
***
wildtype
Gnat1-/-
Optomotor Response
c
Contrast sensitivity
n = 4
No OR
n = 12
d
Acuity (cycles / degre)
Intrinsic Imaging of V1
b
Stim 1
Stim 2
Stim 3
Stim 4
Combined
Stimulus
Wildtype
Gnat1-/-
Watermaze
e
% correct choices made
Unable to complete task
n = 21
f
g

Supplementary Figure S2. Normal visual function is maintained under photopic but absent under scotopic conditions in the non-injected *Gnat1*$^{-/-}$ mouse. a, Mean photopic b-wave amplitudes from flash ERG recordings performed at 0.007 and 10 cds/m^2 on wildtype (*black bars*) and *Gnat1*$^{-/-}$ *(grey bars*) mice. **b**, Optical intrinsic imaging of wildtype and *Gnat1*$^{-/-}$ mouse visual cortex under scotopic and photopic conditions. Different visual stimuli (i) elicited distinct optical signals in different regions of V1 in both wildtype and *Gnat1*$^{-/-}$ eyes under photopic conditions (iv, v, respectively), but only in wildtype mice under scotopic conditions (iii, iv, respectively). *Far right,* Overlapping parts of the 4 stimuli were colour-coded (i). Only responses present for two overlapping stimuli were considered a genuine sensory-evoked signal and represented with the corresponding colour (ii-vi). Colour saturation is proportional to amplitude of responses (black = no response). Black arrows indicate the approximate posterior-to-anterior axis of the brain (see Fig. 2d). Scale bars=1mm; $\Delta I/I$=relative intensity values. **c, d**, Mean photopic contrast sensitivity and visual acuity threshold measurements for wildtype (*black bars*) and *Gnat1*$^{-/-}$ (*grey bars*) mice, as assessed using Optomotry™. **e-g,** Mean pass rate (**e**), contrast sensitivity (**f**) and visual acuity (**g**) for wildtype (*black bars*) and *Gnat1*$^{-/-}$ (*grey bars*) mice, as assessed using the watermaze test.

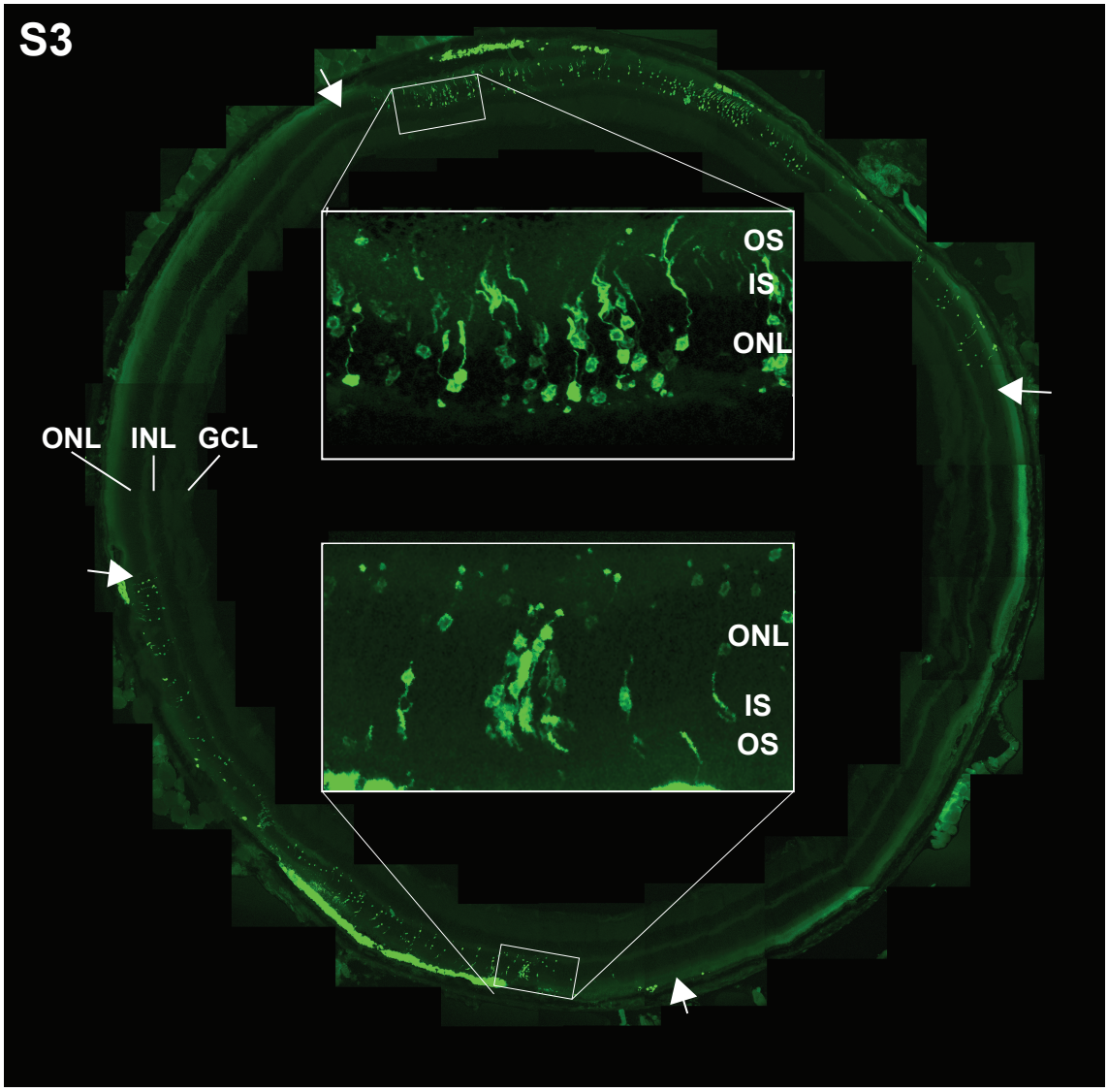
S3
OS
IS
ONL
ONL
INL
GCL
ONL
IS
OS

Supplementary Figure S3. Integration in the adult *Gnat1*$^{-/-}$ retina. Montage from 10μm section showing spread of integration (arrows) of *Nrl.GFP*$^{+ve}$-rods (*green*) in relation to the two injection sites.

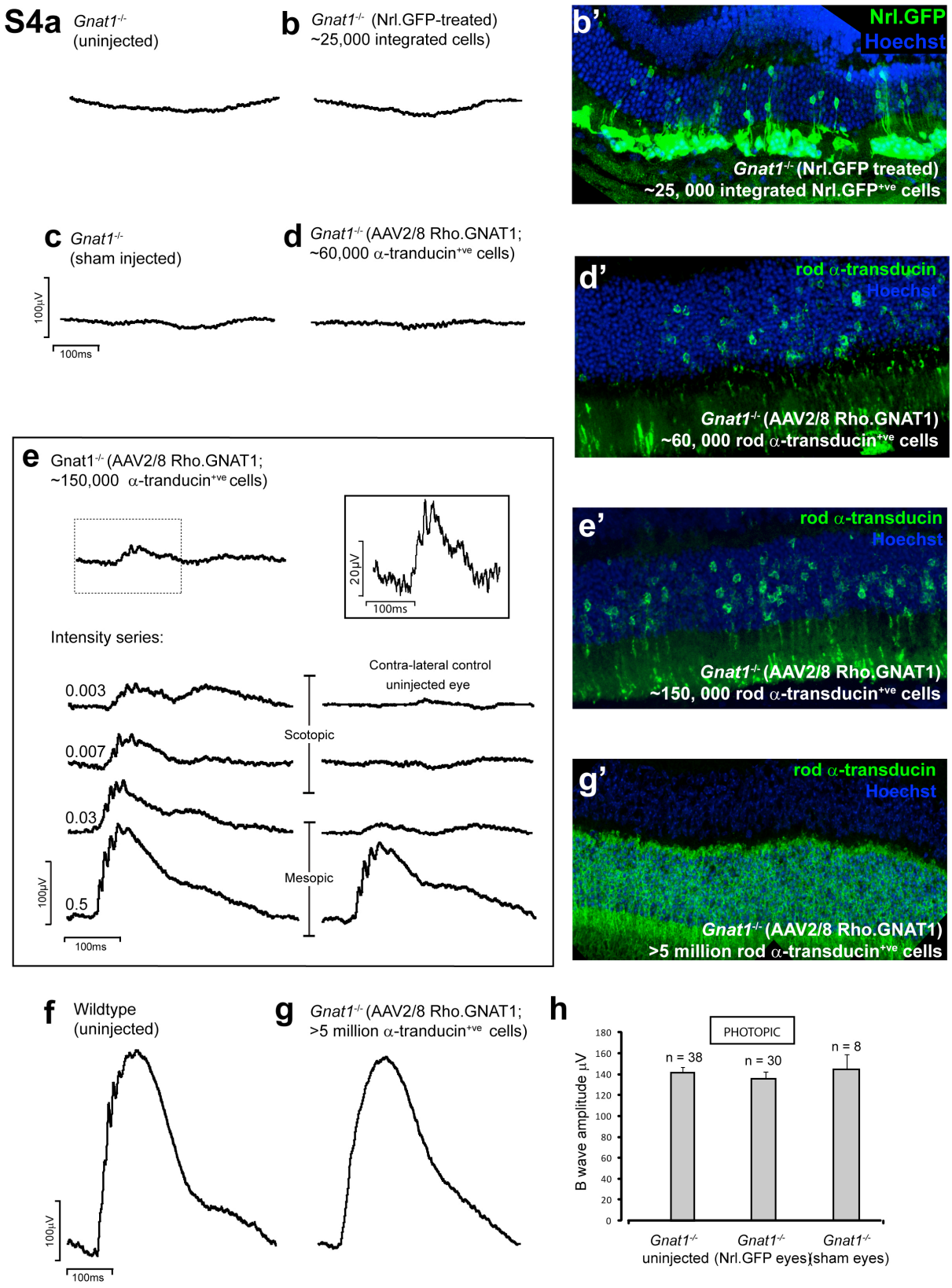
S4a
Gnat1-/- (uninjected)
b
Gnat1-/- (Nrl.GFP-treated) ~25,000 integrated cells)
b'
Nrl.GFP
Hoechst
Gnat1-/- (Nrl.GFP treated)
~25, 000 integrated Nrl.GFP+ve cells
c
Gnat1-/- (sham injected)
d
Gnat1-/- (AAV2/8 Rho.GNAT1; ~60,000 α-tranducin+ve cells)
100μV
100ms
d'
rod α-transducin
Hoechst
Gnat1-/- (AAV2/8 Rho.GNAT1)
~60, 000 rod α-transducin+ve cells
e
Gnat1-/- (AAV2/8 Rho.GNAT1; ~150,000 α-tranducin+ve cells)
20μV
100ms
Intensity series:
Contra-lateral control uninjected eye
0.003
0.007
0.03
0.5
Scotopic
Mesopic
100μV
100ms
e'
rod α-transducin
Hoechst
Gnat1-/- (AAV2/8 Rho.GNAT1)
~150, 000 rod α-transducin+ve cells
g'
rod α-transducin
Hoechst
Gnat1-/- (AAV2/8 Rho.GNAT1)
>5 million rod α-transducin+ve cells
f
Wildtype (uninjected)
g
Gnat1-/- (AAV2/8 Rho.GNAT1; >5 million α-tranducin+ve cells)
100μV
100ms
h
PHOTOPIC
B wave amplitude μV
180
160
140
120
100
80
60
40
20
0
n = 38
n = 30
n = 8
Gnat1-/-
Gnat1-/-
Gnat1-/-
uninjected (Nrl.GFP eyes)
sham eyes)

Supplementary Figure S4. ERGs in the non-injected and transplanted *Gnat1*$^{-/-}$ mouse. a-c, Typical dark-adapted scotopic (0.007 cds/m^2) ERG traces recorded at 4 weeks post-injection in **a,** non-injected *Gnat1*$^{-/-}$ mice, **b**, *Gnat1*$^{-/-}$ mice with 25,000 integrated *Nrl.GFP*$^{+ve}$-rods, or **c**, *Gnat1*$^{-/-}$ mice receiving *Gnat1*$^{-/-}$ cell (sham) injections. **b',** representative image of integrated *Nrl.GFP*$^{+ve}$-rods from retina shown in (b). **d, e, g,** Typical dark-adapted scotopic ERG traces recorded at 4 weeks post-injection in *Gnat1*$^{-/-}$ mice receiving dual injections of different doses of AAV2/8.Rho.GNAT1, which resulted in 60, 000 (**d'**), 150, 000 (**e'**) and >5 million (**g'**) rod α-transducin^{+ve} cells, respectively (as determined by immunohistochemistry and fluorescence microscopy; representative images shown). **f**, ERG trace recorded under the same conditions in non-injected wildtype control mice. A robust, ERG was observed (with intensity series) in animals with 150, 000 transduced cells, but not 60, 000 transduced cells. h, Mean photopic b-wave amplitudes from flash ERG recordings performed at 10 cds/m^2 on Gnat1$^{-/-}$ mice receiving *Nrl.GFP*$^{+ve}$-rods (*green bars*) or *Gnat1*$^{-/-}$ cell (sham) (*dark grey bars*) injections.

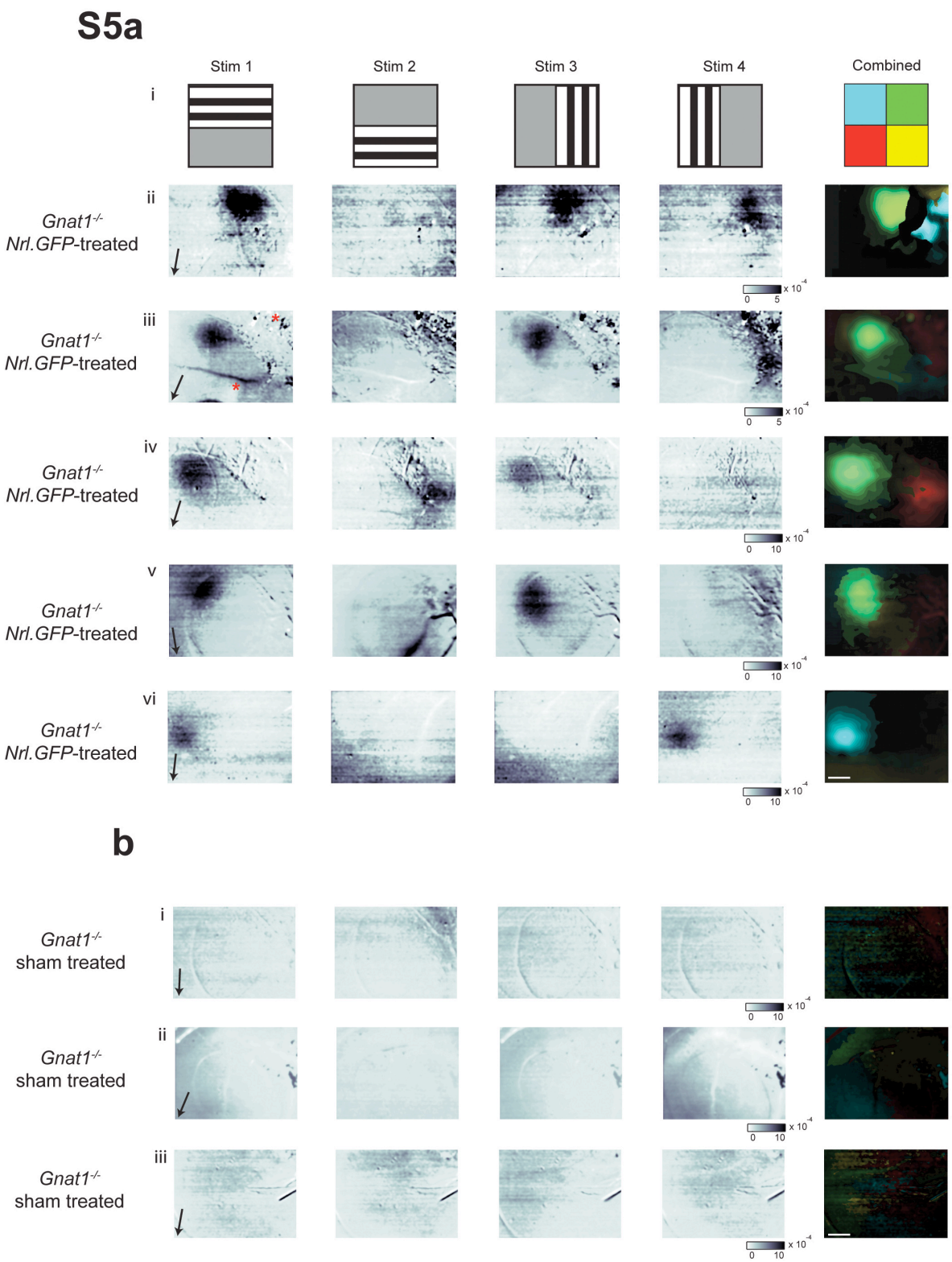
S5a
Stim 1
Stim 2
Stim 3
Stim 4
Combined
i
ii
Gnat1-/-
Nrl.GFP-treated
iii
Gnat1-/-
Nrl.GFP-treated
iv
Gnat1-/-
Nrl.GFP-treated
v
Gnat1-/-
Nrl.GFP-treated
vi
Gnat1-/-
Nrl.GFP-treated
x 10-4
0 5
0 10
b
i
Gnat1-/-
sham treated
ii
Gnat1-/-
sham treated
iii
Gnat1-/-
sham treated

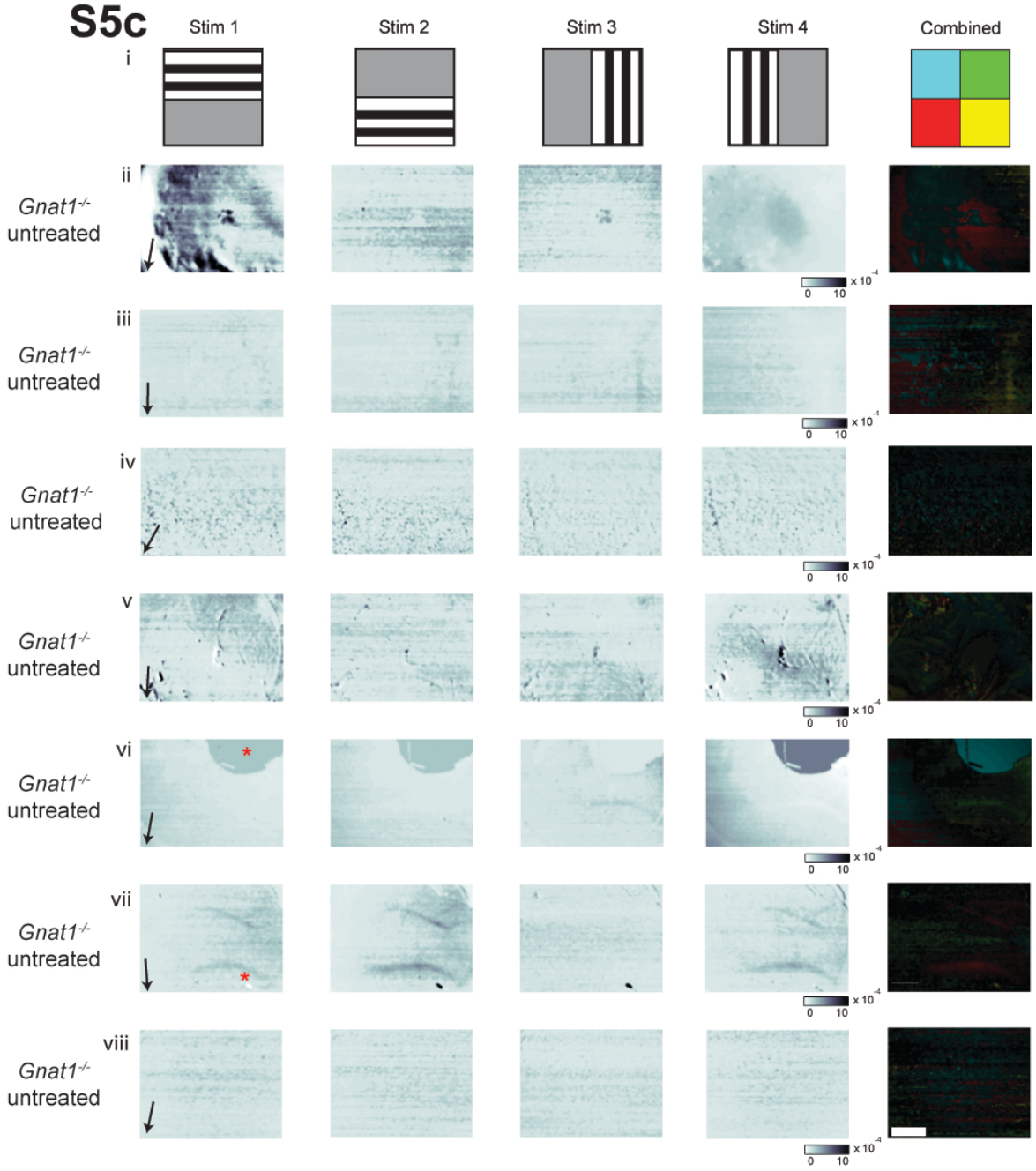
S5c
Stim 1
Stim 2
Stim 3
Stim 4
Combined
i
ii
Gnat1-/-
untreated
iii
Gnat1-/-
untreated
iv
Gnat1-/-
untreated
v
Gnat1-/-
untreated
vi
Gnat1-/-
untreated
vii
Gnat1-/-
untreated
viii
Gnat1-/-
untreated
x 10-4
0 10

Supplementary Figure S5. Optical intrinsic imaging of transplanted and control *Gnat1*$^{-/-}$ mouse visual cortex. a, *Left*, Raw data: the visual stimuli (i) elicited distinct optical signals in V1 in all 5 *Gnat1*$^{-/-}$ eyes receiving *Nrl.GFP*$^{+ve}$-rod-precursor transplants (ii-vi). Not all stimuli elicited a response in all animals. *Far right,* Overlapping parts of the 4 stimuli were colour-coded (i). Only the response present for two overlapping stimuli was considered a genuine sensory-evoked signal and represented with the corresponding colour (ii-vi). The colour saturation is proportional to the amplitude of the responses (black = no response). **b, c,** No signal was observed following presentation of the same stimuli to sham-injected (**b**ii-iv) or untreated (**c**ii-iv) *Gnat1*$^{-/-}$ eyes. No signal was seen in the absence of any visual stimulus (data not shown). Black arrows indicate the approximate posterior-to-anterior axis of the brain (see Fig. 2d). Examples of imaging artefacts are indicated by asterisks (*red*), including connective tissue (a iii), veins (a iii, cv ii) and camera saturation (c vi). Scale bars = 1mm; $\Delta I/I$=relative intensity values. N.B. *Nrl.GFP*-transplanted animal no. 1 (a ii), *Gnat1*$^{-/-}$- injected animal no. 2 (b iii) and *Gnat1*$^{-/-}$ untreated animal no. 2 (c iii) are shown post-filtering (see Supplementary Information) in Fig. 2e and Supplementary Fig. S2b

SUPPLEMENTARY METHODS

Animals

C57BL6 (Harlan, UK), *Nrl.GFP*$^{+/+}$ (A. Swaroop, University of Michigan, USA)[7] and *Gnat1*$^{-/-}$ (J. Lem, Tufts University School of Medicine, USA)[2] mice were maintained in the animal facility at University College London. Adult (male and female) recipient animals were 6-8 weeks old at the time of transplantation. All experiments have been conducted in accordance with the Policies on the Use of Animals and Humans in Neuroscience Research, revised and approved by the ARVO Statement for the Use of Animals in Ophthalmic and Vision Research. Animals were kept on a standard 12/12 hour light-dark cycle and all assessments of visual function were conducted in the first 8 hrs of the light phase.

Dissociation of retinal cells and transplantation

Surgery was performed under direct ophthalmoscopy through an operating microscope, as previously described [1, 3-5]. Recipient mice were anaesthetised with a single intra-peritoneal injection of 0.15 ml of a mixture of Dormitor (1 mg/ml medetomidine hydrochloride, Pfizer Pharmaceuticals, Kent, UK), ketamine (100 mg/ml, Fort Dodge Animal Health, Southampton, UK) and sterile water for injections in the ratio of 5:3:42.

Dissociated cells were prepared from P1 or P4-8 *Nrl.GFP*$^{+/+}$ mice, as described previously [4,5]. Cells were dissociated using a papain-based kit (Worthington Biochemical, Lorne Laboratories UK) according to manufacturer's instructions and FACS sorted for GFP fluorescence using a MoFlo XDP cell sorter. Sorted *Nrl.GFP*$^{+ve}$ cells were collected in EBSS containing 20 % FCS, spun at 100 G for 10 mins and the resulting pellet re-suspended at 200, 000 live cells / μL (as assessed using a Scepter hand-held cell counter; Millipore, UK) in sterile EBSS and DNase (0.005%) and kept on ice prior to

transplantation. Prior to subretinal injection of donor cells, the tip of a sterile 8mm, bevelled, 34-gauge hypodermic needle (Hamilton, Switzerland) was inserted through the sclera, at the level of the temporal region of the anterior chamber and slowly withdrawn. This creates a reproducible release of pressure within the eye. A small amount of air (0.6 μl) was drawn up into a sterile needle (as before) before loading with cells. The needle was inserted tangentially through the sclera and RPE into the sub-retinal space. Cell suspensions were slowly injected (1 μl per injection) into both the superior and inferior retina to produce two retinal detachments (Supplementary Fig. S1a).

Immunohistochemistry and confocal microscopy

Animals were sacrificed by cervical dislocation. Eyes were quickly removed and dissected in 4 % paraformaldehyde (PFA) in PBS. Eye cups were prepared and fixed for 15 – 60 mins in PFA, cryoprotected in 20 % sucrose/PBS, cryoembedded in OCT (RA Lamb, Eastborne, UK) and cut as transverse sections 20 μm thick. Retinal cryosections were air-dried for 15 - 30 mins and washed in PBS. For immunohistochemistry, sections were pre-blocked in PBS containing normal goat serum (2 %), bovine serum albumin (1 %) and 0.05 % Triton-X 100 for 1 hr before being incubated with primary antibody [rod α-transducin (1:500; Santa Cruz); Bassoon (1:2000; mouse-monoclonal; Stressgen); dystrophin (Novacastra); RIBEYE (CtBP2; 1:500; mouse monoclonal; BD Biosciences; N.B. RIBEYE is composed of a unique A-domain specific for ribbons, and a B-domain that is, with the exception of the first 20 amino acids, identical to the transcriptional corepressor CtBP2. Both RIBEYE and CtBP2 are derived from the same gene; PKC-α (AbCam)] overnight at 4 °C. After rinsing 3 x 10 mins with PBS, sections were incubated with the appropriate Alexa-tagged secondary antibody (Invitrogen Molecular Probes) for 2 hrs at room temperature (RT), rinsed and counter-stained with Hoechst 33342 (Sigma-Aldrich, Gillingham, UK). Negative controls omitted the primary antibody.

Retinal sections were viewed on a confocal microscope (Leica TCS SP2). Unless otherwise stated, images show merged confocal fluorescence images of projection images of an xyz stack through a retinal section, ~10 μm thick.

Cell counts

Cells were considered to be integrated if the whole cell body was correctly located within the outer nuclear layer, and at least one of the following was additionally visible; spherule synapse, inner/outer processes, inner/outer segments. The average number of integrated cells per eye was determined by counting all integrated GFP^{+ve} cells in alternate serial sections through each eye and doubling that number. Animals were omitted from quantification analysis only if there was clear evidence of an injection occurring intravitreally, rather than subretinally, or if no cell mass was evident in the subretinal space at the time of counting, an indication that complete reflux of the donor cell suspension had occurred at the time of injection (typically <5 % of injections) or if eyes demonstrated evidence of significant inflammation, as described previously [4,5].

For AAV2/8 Rho.GNAT1 experiments (below), mice were light-adapted for 30 mins to ensure translocation of rod α-transducin into the cell body [10], before being sacrificed and the eyes embedded. The average number of rod α-$transducin^{+ve}$ cells was determined by taking serial sections 15 μm thick and staining for rod α-transducin (as above), before every 3^{rd} section was assessed and the number of rod α-$transducin^{+ve}$ cells counted. This number was then trebled to give an estimate of the mean number of rod α-$transducin^{+ve}$ cells per eye.

Electron Microscopy

For both immunolocalization and ultrastructural analyses, anesthetized animals were transcardially perfused through the ascending aorta with (1) 10 ml of heparin saline (1,000 units/ml), (2) 20 ml of 4% PFA/3.75% acrolein (Polysciences, Warrington, PA) in 0.1 M phosphate buffer (pH 7.4), (3) 60 ml of 4% PFA in 0.1 M phosphate buffer. The eyes were subsequently enucleated and prepared for eye cups. The eye cups were further fixed in 4% PFA/ 0.1% glutaraldehyde in 0.15 M cacodylate buffer (pH 7.4) overnight prior to the agarose embedding and vibratome sectioning. Immunolabeling was

carried out using free-floating methods previously described[23]. All immunolabelled sections were examined by a Leica TCS SP2 microscope with a HCX PL APO 63X/1.4 Oil CS Blue objective using Leica Confocal Software (Nussloch, Germany). For ultrastructural analysis, retinal sections were permeabilized by the "freeze-thaw" method, immunolabelled, and post-fixed with 2% glutaraldehyde for 10 min after the secondary antibody incubation, as described previously. The immunolabeled sections were processed for silver-enhancement, OsO4 fixation, and dehydration. Finally, the sections were then flat embedded in Epon, and further cut into 70-nm thick ultrathin sections. The most superficial sections were counterstained and examined on a Philips CM10 electron microscope. Negative controls were treated identically and in parallel except that primary antibodies were omitted. In some experiments, conventional EM was carried out using the same procedures except that the immunolabeling steps were omitted. It is not possible to provide fully quantitative assessment of synapse formation via immuno-EM; it is difficult to identify sections in which transplanted cell synapses are both sufficiently labelled and in perfect alignment with the plane of sectioning. Estimates are given on the basis of the cells that could be identified that fulfilled these criteria.

Suction-pipette recordings

Mice were dark-adapted overnight, anesthetized by Avertin, and enucleated before euthanasia. Each eye was hemisected and the retina removed. The retina, with 3-4 radial cuts around the periphery, was flat-mounted photoreceptor-side up on a GSTF Millipore filter paper and placed in bicarbonate-buffered Ames medium (Sigma-Aldrich) before being chopped into 100-μm slices with a custom-built tissue chopper. The retinal slices together with the underlying filter paper were transferred and mounted sideways in the recording chamber. All procedures were performed in infrared or dim-red light.

Recordings were carried out at physiological temperature, ~35-37 °C, on a Zeiss upright microscope with infrared DIC optics and imaging. The bath solution (bicarbonate-buffered Ames medium equilibrated with 5% CO_2/95% O_2) was temperature-controlled and run at ~5 ml/min through the 1-ml experimental chamber. Temperature was monitored by a thermistor in the chamber. Integrated *Nrl.GFP*$^{+ve}$-rods were identified by their GFP-fluorescence. Data presented is from *Nrl.GFP*$^{+ve}$-rod-photoreceptors correctly located within the ONL with an intact inner segment, cell body and synaptic terminal. A total of 9 *Nrl.GFP*$^{+ve}$ cells were recorded. The number of cells examined for each group is in parentheses in Figure 2; this cell number per group is not always the same across parameters because not all parameters were obtainable for each cell. We also recorded from non-integrated GFP^{+ve} cells located in the subretinal space and near the RPE: none gave detectable light responses. In order to minimize rhodopsin bleaching during fluorescence-based cell-hunting, excitation light intensity (450-490 nm) was kept low and the GFP signal was visualized with a highly-sensitive EM-CCD camera (Lucas, ANDOR). The image-sampling of the camera was also synchronized with the exciting flash (30 msec). The infrared DIC image of the retinal slice was overlaid with the GFP-fluorescence image to guide the recording pipette. Nonetheless, we found that *Nrl.GFP*$^{+ve}$-rods were desensitized by the GFP-excitation light (63.2 μW 450-490nm, ~1.5 sec in total). Accordingly, for all of the experiments reported here, 100-μM 9-*cis*-retinal (a readily available analog of 11-*cis*-retinal; Sigma) in 1% BSA-Ames solution was run through the chamber for 1 hour in complete darkness before light stimulation of the recorded cell began. Note that the bleaching/regeneration procedure reduced the speed of the dim -flash-response-kinetics and the sensitivity of wildtype rods (see Figure 2b), most likely due to the combined lower quantum efficiency and extinction coefficient of 9-*cis* pigments compared with native 11-*cis* pigments [24,25]. In all cases, the saturated light responses were about half of that recorded directly from the outer segment [26] largely because of the incomplete current-collection due to physical constraints to the suction pipette.

The recording configuration was modified from a previously-described procedure [12,20]. The *Nrl.GFP*$^{+ve}$-rod soma was drawn into a snug-fitting glass pipette with a 3-4 μm opening at its tip and

containing HEPES-buffered Ames solution, which was made from Ames stock (without $NaHCO_3$, Sigma-Aldrich) with additional 10mM HEPES and 15mM NaCl, pH 7.4 by NaOH. The osmolarity was adjusted to 283 mOsm/L by glucose to match the bicarbonate-buffered Ames. The recorded rod was stimulated with an LED light (λ_{max} at 505 nm, with 30-nm bandwidth) delivered through a light guide into the microscope epifluorescence port. The light intensity and duration (10msec) were controlled by custom circuitry. The intensity of the light source was periodically calibrated with a radiometer. In Figure 2a, the flash, delivered at time zero, is indicated by light monitor and flash intensity was 1.1, 8.8, 57, 280, 1403 and 4962 photons μm^{-2} for dark-adapted wildtype; 50, 244, 1,221, 4,318 and 15,973 photons μm^{-2} for bleached/regenerated wildtype rod and 222, 854, 2,675, 9,257, 26,862, 75,701 and 229,766 photons μm^{-2} for bleached/regenerated *Nrl.GFP*$^{+ve}$-rod.

Membrane current was measured with a current-to-voltage amplifier (Axopatch 200B, Axon Instruments). All signals were low-pass filtered at 20 Hz (8-pole Bessel) and sampled at 500 Hz. The response–intensity relationship at the transient peak of the response was fit with the Michaelis equation, $R = R_{max} [I / (I + \sigma)]$, where R is transient-peak response amplitude, R_{max} is saturated peak-response amplitude, I is flash intensity, and σ is the half-saturating flash intensity. Rod sensitivity is inversely proportional to σ. The following parameters were measured: Time-to-peak (the time lapse from flash to transient peak of dim-flash response); the integration time, t_i, of the dim-flash response (a measure of its overall duration, and is given by $t_i = \int f(t)dt/f_p$, where $f(t)$ is the response profile and f_p is its transient-peak amplitude); half-saturating flash intensity (i.e., intensity that elicited a half-maximum response); and σ, which is inversely proportional to sensitivity. Data were analyzed by Origin (Origin Lab Corp.) and presented as mean ± S.E.M, with the exception of sensitivity (σ). This is presented as median + range due to it being IC_{50} data and has thus been logarithm transformed.

The LED light source was converted to “equivalent” monochromatic light with the λ_{max} of the respective visual pigment for data analysis and display. For rods without bleaching, the LED light was

converted to equivalent 498nm light, the λ_{max} of 11-*cis*-rhodopsin. The GFP epifluorescence-excitation light (see above) bleached over 99.9% rhodopsin (calculated by equation in [26]. So for bleached/regenerated rods, the light was converted to equivalent 485nm light, the λ_{max} of 9-cis-rhodopsin. The conversion was done by using the normalized action spectrum of rhodopsin, $f(\lambda)$, with λ_{max} of 498nm and 485nm, respectively, and the power-scaled spectrum of the LED light, $L(\lambda)$. The conversion ratio is:

$Power_{equivalent\ \lambda_{max}\ light} = Power\ ratio \times Power_{light\ with\ L(\lambda)\ spectrum}$, where

$$Power\ ratio = \frac{\frac{hc}{\lambda_{\max}}\int\left(\frac{L(\lambda)}{hc/\lambda}\times f(\lambda)\right)d\lambda}{\int L(\lambda)\,d\lambda} = \frac{\int\left(\lambda \times L(\lambda)\times f(\lambda)\right)d\lambda}{\lambda_{\max}\int L(\lambda)\,d\lambda}$$

Plasmid construction and production of recombinant AAV 2/8

Murine *GNAT1* cDNA followed by a polyadenylation site was enzymatically digested and extracted from the CMV-*GNAT1*.SPORT6 plasmid (Source Bioscience, Cambridge UK). This cassette was cloned into pD10 containing the rhodopsin promoter and AAV-2 inverted terminal repeat (ITR) sequences to form the construct pD10/Rho-*GNAT1* (total length 8230 bp). The construct was verified by sequencing. Recombinant AAV2/8 serotype particles were produced through a tripartite transfection method into HEK293T cells. AAV8 packaging, helper and pD10/Rho-*GNAT1* plasmids were combined with polyethylenimine (PEI, Polysciences, Inc., Eppelheim, Germany) and left to form complexes for 10 minutes. The mixture was added to HEK293T cells and left for 24 hours. The cells were harvested and concentrated 2 days after transfection and lysed using repeated freeze/thaw cycles to release the viral particles. HEK293T cell nucleic acid components were removed by Benzonase (Sigma Aldrich, Dorset, UK) treatment and virus preparation was cleared of cellular debris by multiple centrifugation steps, followed by purification using ion exchange chromatography. The virus preparation was concentrated using a Vivaspin 4 concentrator (10 kDa, Sartorius Stedim Biotech,

Fisher Scientific, Loughborouh, UK), to 100 – 150 µl. Viral particle titres were determined using dot-blot analysis of purified virus DNA and plasmid controls of known concentrations.

Assessment of scotopic recording conditions

Scotopic conditions were determined experimentally based on cited thresholds. Light levels were measured using an IL1700 photometer and adjusted using neutral density filters, where appropriate. The literature indicates that light levels less than 0.01 cds/m^2 can be considered as scotopic conditions for the murine retina [27,28]. It is important to note, however, that scotopic thresholds in behavioural tests can differ, depending upon the test used. Therefore, we also confirmed that although we could reliably induce responses from wildtype mice, there was no response from untreated *Gnat1*$^{-/-}$ control mice. This was established for each experimental test (and corresponded to a light level of 0.007 cds/m^2 or less). On no occasion could we record responses from any non-injected (or sham injected) control *Gnat1*$^{-/-}$ mice under the scotopic lighting conditions that were used.

Electroretinograms

ERGs were recorded prior to and 3, 4, 5 & 6 weeks after injection of *Nrl.GFP*$^{+ve}$-rod-precursors or AAV2/8 Rho-GNAT1, using an Espion E^2 system with a ColourDome stimulator (Diagnosys LLC, Lowell, MA). For the transplantation experiments, test eyes received superior and inferior subretinal injections of 200, 000 FACS-sorted *Nrl.GFP*$^{+ve}$-rod-precursors. The contralateral control eye received an identical sham cell injection, but containing cells from an age-matched *Gnat1*$^{-/-}$ donor or remained un-treated. For the AAV2/8 experiments, test eyes received dual subretinal injections of AAV2/8 Rho-GNAT1 at 10^9, 10^7 or 10^5 viral particles/injection. The contralateral control eye was left un-treated.

A masked protocol was employed such that the person performing the ERGs and analysis did not know which eye received sham and which eye received *Nrl.GFP*$^{+ve}$-rod-precursor-cells. Animals were

dark-adapted overnight and all subsequent procedures were performed under dim red light. Animals were anaesthetized as above and kept warm with a thermostatically controlled heat wrap linked to a body-temperature probe. The pupils were dilated using Tropicamide 1%. Viscotears were placed on each cornea to keep it moistened after corneal contact electrodes and midline subdermal reference and ground electrodes were placed. Animals were left for a further 10 minutes in complete darkness prior to recording. Ganzfeld ERGs were obtained simultaneously from both eyes to provide an internal control. Single flash recordings were obtained at light intensities of 0.003, 0.007, 0.03, 0.5 and 3 cds/m^2 using a sampling frequency of 5 kHz, a flash duration of 4 ms, and a frequency stimulus of 0.5 Hz. Data were recorded from 10 ms before stimulus onset to 400 ms post-stimulus. The bandpass filter was set between 0 and 1 kHz. Ten responses per intensity level were averaged with an interstimulus interval of 10 s (0.003, 0.007, and 0.03 cds/m^2) or a 20 s interstimulus interval (0.5 and 3 cds/m^2). For analysis, the a- and b-wave amplitudes (a-wave trough to b-wave peak) of the treated eyes were paired with the contralateral eyes. This method controls for interanimal and intertest variance. Since no a- or b-wave is observable under scotopic conditions in the *Gnat1*$^{-/-}$ mouse, we used wildtype mice to provide a guide for the expected timing of any b wave following transplantation. The mean time to peak for wildtype mice (n = 3) was determined for each intensity and this time point used to determine a- and b- wave amplitudes of *Gnat1*$^{-/-}$ mice.

Optical imaging

Mouse visual cortical haemodynamic responses ("intrinsic signals") were recorded using the method developed by Grinvald et al [13]. Mice were dark-adapted overnight. Immediately prior to the experiment, mice were anesthetized with Ketamine/Dormitol and mounted in a stereotaxic frame. Tropicamide was applied to both eyes and Viscotears was constantly re-applied throughout the experiment to keep the eyes moist. The scalp covering the occipital cortex contralateral to the stimulated eye was resected. A circular metal headplate was secured to the skull and a glass

coverslip was positioned within the ring on the exposed skull. Lambda and bregma were used as reference points to ensure the headplate was placed correctly, allowing imaging of a large cortical area (5 mm x 5 mm) encompassing several visual areas including V1, the auditory cortex (Au) and Somatosensory cortex (S1)(see Fig. 2d.). The anterior-posterior axis of the brain is marked on all images with an arrow (*black*). Images shown in Fig. 2e and Supplementary Fig. 2b are cropped from the larger raw data sets shown in Supplementary Fig. S4. Intrinsic signals were acquired under red light (660-nm) using a CMOS camera (MV-D1024E-160-CL, Photonfocus AG) running at 10Hz and custom software. Two 50 mm Nikkor lenses were used in a macroscope configuration with 1:1 magnification. Visual stimuli were presented in the contralateral visual field on two LCD monitors (60 Hz refresh rate) positioned ~30cm in front of the animal (Fig. 2). Stimuli consisted of a series of either horizontal or vertical black and white bars and were presented inside four rectangular windows tessellating the contra-lateral visual field. Two partially-overlapping vertical windows (50 deg width, 60 deg height) covered 90 deg of azimuth (0 to 90 deg), and two horizontal windows (90 deg width, 30 deg height) covered 60 deg of elevation (-10 to +50 deg). The stimuli inside the windows were vertical square-wave gratings (0.03 cycles/^{o}, 100% contrast) whose contrast reversed sinusoidally (2 Hz frequency, 3 s duration). A blank stimulus (0% contrast, i.e. grey screen) was presented with the same duration. The four stimuli and the blank were presented 15 to 20 times in random order. The experiment was repeated for both eyes, with one eye covered while the other was stimulated. Except where otherwise stated, stimulus intensity was low (<0.0007 cds/m^2), to test vision in the scotopic range. Stimulus intensity was controlled by covering the screens with neutral density filters. Scotopic conditions were determined using unprocedured *Gnat1*$^{-/-}$ and wildtype mice to ascertain the precise threshold between photopic and scotopic vision under these experimental conditions. Recordings under photopic conditions were taken where possible as a positive control after scotopic conditions.

Maps of haemodynamic responses for each stimulus condition were obtained from image frames acquired for 3 seconds after stimulus offset. First, averaged maps were obtained by taking the mean

over time and over stimulus repetitions. Each map was then divided by its grand-average (over space and time) thus to obtain relative intensity values ($\Delta I/I$). Finally, correction for uneven illumination and reflectance was made by subtracting the response to the blank stimulus (a grey screen). Unless otherwise stated, the resulting maps were blurred in space with a 2D Gaussian filter (σ= 52μ) to remove pixel noise. These intensity maps were multiplied by a wide 2-D Gaussian window with unit amplitude (sigma = 100 pixels, 1.4 mm) to reduce artefacts at the borders of the window.

Combined colour-coded maps of retinotopy were obtained by arranging the four stimuli as describing a rotation around the centre of the screen, with stimuli 1, 3, 2, and 4 covering the top, right, bottom, and left of the screen. For each pixel we considered the four responses to this sequence of stimuli and fitted it with a sinusoid. The phase of the sinusoid indicates the preferred quadrant, and is indicated in each pixel by the colour hue. Colour saturation represents the strength of the responses and is the average response to the two stimuli covering the preferred position.

Optomotor Response

Contrast sensitivities and visual acuities of treated and untreated eyes were measured by observing the optomotor responses of mice to rotating sinusoidal gratings (OptoMotry^{TM}) [9,15,16]. Mice reflexively respond to rotating vertical gratings by moving their head in the direction of grating rotation. The protocol used yields independent measures of the acuities of right and left eyes based on the unequal sensitivities of the two eyes to pattern rotation: right and left eyes are most sensitive to counter-clockwise and clockwise rotations, respectively. A double-blind two alternative forced choice procedure was employed, in which the observer was "masked" to both the direction of pattern rotation and to which eye received *Nrl.GFP*$^{+ve}$-rod-precursors or *Gnat1*$^{-/-}$ cells. Briefly, each mouse was placed on a pedestal located in the centre of four inward facing LCD computer monitors

screens and was observed by an overhead infrared video camera with infrared light source. Once the mouse became accustomed to the pedestal a 7s trial was initiated by presenting the mouse with a sinusoidal striped pattern that rotates either clockwise or counter-clockwise, as determined randomly by the OptoMotry^{TM} software. Involuntary reflex head tracking responses are driven by the left (clockwise rotations, *black arrow* in Fig. 3a) and right (counter-clockwise rotations, *white arrow* in Fig. 3a) eyes, respectively. Visual acuity and contrast sensitivity were measured under scotopic conditions (<0.003 cds/m^2) as determined using unprocedured *Gnat1*$^{-/-}$ and wildtype mice to determine the precise threshold between photopic and scotopic vision under our experimental conditions. The observer selected the direction of pattern rotation based on the animal's optomotor response and the monitors returned to 50% gray until the next trial. Contrast sensitivity was measured at a spatial frequency of 0.064 cycles/° and at a speed of rotation of 0.75 Hz. These settings have previously reported as optimal spatial and temporal frequencies for maximal stimulation in wildtype mice under scotopic conditions [9]. In order to assess visual acuity, gratings had a constant contrast of 100%. Using a staircase paradigm the program converges to measures of the acuities or contrast sensitivity of both eyes defined as the spatial frequency or % contrast yielding ≥ 70 % correct observer responses. Acuity was defined as the highest spatial frequency yielding a threshold response. Similarly, contrast sensitivity was defined as 100 divided by the lowest percent contrast yielding a threshold response. Animals were dark adapted over night and visual acuities and contrast sensitivities were measured for both eyes of each mouse at least three times before and after (4-6 weeks) cell transplantation on independent days. Animals were sacrificed after assessment and the number of correctly integrated cells determined. While this protocol permits the separation of right and left eye sensitivities, the contralateral eye is not 'blind' to the stimulus. However, controls in which both eyes received sham injections of *Gnat1*$^{-/-}$ cells confirmed the absence of any optomotor response (n=4). This demonstrates that any small improvements seen in the "sham" eyes of the test animals were due to cross-talk from the treated eye. Control measurements under photopic conditions before and after transplantation were included as positive

controls. Animals were light adapted (60 cds/m^2) for 30 min prior to testing and the initial stimulus was a 0.200 cycles/degree sinusoidal pattern with a fixed 100% contrast. For photopic contrast sensitivity measurements, the initial pattern was presented at 100% contrast, with a fixed spatial frequency of 0.128 cycles/degree. Visual acuity and contrast sensitivity were measured under photopic conditions (60 cds/m^2).

Watermaze

The water maze task is an effective means of measuring visual ability in rodents [17]. Visual function was assessed after training to discriminate between a neutral stimulus and a grating displayed pseudo-randomly on 2 separate computer monitors at one end of a Y-shaped water tank (see Fig. 4a). The two computer monitors (Mitsubishi Diamond Plus 7458, 17") were positioned side by side facing into the tank with the bottom of the screens at the water level. Screen brightness was calibrated and adjusted so that they were equal. Animals were trained under photopic conditions (30 log cd/m^2) to swim towards the monitors and associate a low frequency grating with a submerged hidden platform that allows them to escape from the water. Their ability to find the platform indicates their capability to resolve the visual task. The end of the midline divider that separates the stimuli was considered the decision point and the first crossing of this line was scored (pass or fail), irrespective of whether the mouse reached the platform. Swim time latencies were recorded from the time the animal left the delivery channel to the time it reached the platform. Animals were trained to distinguish a vertical grating from a uniform grey level of equal average luminance. Each session consisted of 10 trials presented in a pseudo-random pattern, LRLLRLRRLR (L-Left monitor, R- Right monitor) and animals were considered to have learned the task when they achieved a pass rate of 70 % or higher over the previous 30 trials. All the animals assessed managed to learn this task within 1–3 weeks. Four groups of animals were assessed: 1) *Gnat1*$^{-/-}$ mice receiving

dual injections of *Nrl.GFP*$^{+ve}$-rod-precursors to both eyes, 2) *Gnat1*$^{-/-}$ mice receiving dual injections of age-matched *Gnat1*$^{-/-}$ cells to both eyes, and non-injected 3) *Gnat1*$^{-/-}$ and 4) age-matched *C57Bl/6* wildtype control mice. Animals continued to receive photopic maintenance training throughout the 3 week interval between transplantation and testing (regardless of having received cells or not) and in between scotopic test sessions to ensure good task recall. Pass rates under photopic conditions remained at ≥70 % throughout the experiment, with a small temporary drop in pass rate in the 2 weeks immediately after injections. For scotopic testing, all animals were dark adapted over night and tested on at least three separate days. As visual acuity is poorer under scotopic conditions [9], animals were tested using a grating of 0.086 cycles/°. All spatial frequencies are calculated with respect to the decision point. Scotopic visual acuities and contrast sensitivities were measured for the *Nrl.GFP*-treated animals that performed >70% in the standard conditions and compared to wildtype controls. Each mouse was tested at least three times for each measure. The maze was viewed via infrared lighting and a night vision video camera and the tester was masked to the treatment received by individual animals until after testing was complete and the eyes had been assessed for cell integration. Control photopic recordings were taken in between and two days after the final scotopic testing as a positive control. Animals were light adapted (>60 cds/m^2) for 30 min prior to testing.

Statistics

All means are ± standard error, unless otherwise stated. n = number of animals, eyes, or cells examined, as appropriate. Statistical significance was assessed using Graphpad Prism 5 software, and applying paired t-test, ANOVA with Tukey's or Dunnett's correction for multiple comparisons, Kruskal Wallis or a Fisher's exact test (2-tailed), where appropriate.

Supplementary Movie Legend. Watermaze test for rod-mediated vision. Examples of swimming behaviour in non-injected C57BL/6 wildtype and *Gnat1*$^{-/-}$ controls, *Gnat1*$^{-/-}$ mice receiving *Gnat1*$^{-/-}$ cell (sham) injections and *Gnat1*$^{-/-}$ mice receiving *Nrl.GFP*$^{+ve}$-rod-precursors, tested under scotopic conditions. The mice shown in these movies are identified in *red* on Figure 4b. Mice were trained under photopic conditions to associate a striped grating with a platform allowing escape from the water. All mice could correctly solve the task on >70% of occasions under these conditions. All wildtype mice continued to successfully complete the task under scotopic conditions, swimming quickly and directly to the screen displaying the striped grating (clip 1). Non-injected (clip 2) and sham-injected (clip 3) *Gnat1*$^{-/-}$ controls mice performed no better than chance (50% correct). Swimming behaviour was characterised by indecision, swimming in circles and frequent incorrect choices being made. Conversely, 4/9 of the *Nrl.GFP*-treated *Gnat1*$^{-/-}$ mice were able to complete the task on ≥70% of occasions under scotopic conditions. One of the best examples is shown in clip 4. Swimming behaviour was characterised by significantly shorter swim time latency, compared with *Gnat1*$^{-/-}$ control groups, with animals frequently swimming directly to the correct side. These animals were also quick to rectify any mistakes made (evident in the shorter swim time latencies). As these movies were filmed under infrared lighting conditions, which do not resolve the gratings displayed on the monitors, pseudo gratings have been added post-hoc to show which monitor displayed the grating in any given trial.

Reference List

[23] J. Z. Chuang, Y. Zhao, and C. H. Sung, SARA-regulated vesicular targeting underlies formation of the light-sensing organelle in mammalian rods, Cell **130**, 535-547 (2007).

[24] R. Hubbard and A. Kropf, The Action of Light on Rhodopsin, Proc. Natl. Acad. Sci U. S. A **44**, 130-139 (1958).

[25] V. J. Kefalov*, et al.*, Breaking the covalent bond--a pigment property that contributes to desensitization in cones, Neuron **46**, 879-890 (2005).

[26] D. G. Luo and K. W. Yau, Rod sensitivity of neonatal mouse and rat, J Gen. Physiol **126**, 263-269 (2005).

[27] K. Toda*, et al.*, The electroretinogram of the rhodopsin knockout mouse, Vis. Neurosci. **16**, 391-398 (1999).

[28] M. Cachafeiro*, et al.*, Remaining rod activity mediates visual behavior in adult Rpe65-/- mice, Invest Ophthalmol. Vis. Sci. **51**, 6835-6842 (2010).